

A Study on Dynamic Behavior of Nikken Sekkei Tokyo Building Equipped with Energy Dissipation Systems when Struck by The 2011 Great East Japan Earthquake



15 WCEE
LISBOA 2012

Hiroaki Harada, Tatsumi Shinohara, & Keita Sakakibara

Structural Engineering Department, NIKKEN SEKKEI LTD, Tokyo Japan

SUMMARY:

The Nikken Sekkei Tokyo Building has an energy dissipation system with viscous damping walls and buckling restrained braces. After completion in March 2003, accelerometers were installed and an earthquake observation system was introduced to constantly measure seismic motions with the objective of determining the vibration properties of the building during earthquake (Hiroaki Harada, Masato Ishii, 2005). In this report the properties of the seismic motions and the vibration properties of the building are analyzed and verified using the measured records of the large magnitude 9.0 Great East Japan Earthquake that occurred on March 11, 2011. Also analysis was carried out using the record of an aftershock that occurred after the main earthquake, and the changes in the building's properties after the main shock were confirmed. Displacements of the energy dissipation members were measured. Also, verification was carried out by comparing the design analysis model and the measured results.

Keywords: Energy dissipation system, Earthquake observation, Viscous damping wall, Buckling restrained braces, Response spectra

1. INTRODUCTION

The Nikken Sekkei Tokyo Building is a 60 m high medium high-rise office building with a structural steel energy dissipation structure that was completed in March 2003. The energy dissipation structure has viscous damping walls and low yield point steel buckling restrained braces (Figure 1). In order to determine the vibration properties of the building during an earthquake, accelerometers were installed in the building immediately after completion, and seismic motions were measured and analyzed.¹⁾

Here we report on the results of analysis using the recorded measurements of the main shock of The Great East Japan Earthquake that occurred on March 11, 2011. The Nikken Sekkei Tokyo Building was several hundred kilometers from the epicenter. The oscillations recorded correspond to a medium seismic intensity 5-upper (Japanese seismic scale).

In addition to the 600-second long duration seismic motions of the main shock, many aftershocks were recorded after the main shock. Analysis and verification of the vibration properties of the Nikken Sekkei Tokyo Building was carried out using the records of these earthquakes.

2. DESCRIPTION OF THE BUILDING

The Nikken Sekkei Tokyo Building was designed with a high seismic resistance energy dissipation structure in order to ensure continuation of the main work execution functions even during a major earthquake (Fig. 2). Seismic energy is absorbed by low yield point steel (LY = 100N/mm² class) buckling restrained vibration control braces and viscous damping walls, in order to ensure that there is generally no damage to the structure in a major earthquake (Fig. 4). The main structure is a structural steel moment resisting frame, while columns only have a CFT structure. The energy dissipation braces are designed to absorb energy in medium to large earthquakes, and the viscous damping walls are designed to resist small to medium earthquakes, strong winds, etc.



Figure 1. External view of the building

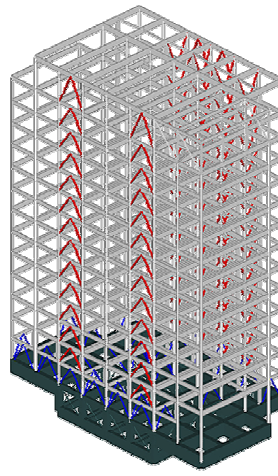


Figure 2. Schematic structural diagram

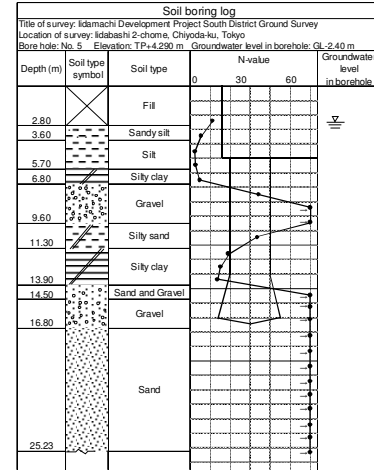
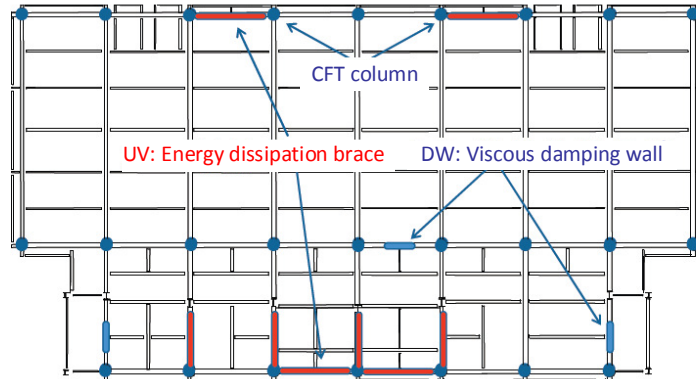


Figure 3. Soil Column Section

S^{*1} grade vibration control structure
(in a major earthquake: no damage (structure remains within the elastic range))



(*1: Seismic resistance grade by Nikken Sekkei)

Design target performance inter-story drift angle
L1(25cm/sec): 1/400~1/300
L2(50cm/sec): 1/200~1/150

Energy dissipation brace
(100N/mm² class)



Viscous damping wall



Figure 4. Structural framing diagram and photos of energy dissipation members

Table 1. Brief description of the building

Location	2-18-3 Iidabashi, Chiyoda-ku, Tokyo
Building area	1,497.75m ² , total floor area: 20,580.88m ²
Number of stories	1-level basement, 14 stories aboveground, 1-level penthouse
Structural type	Aboveground: structural steel (columns only, CFT structure) Basement: structural steel and reinforced concrete structure + reinforced concrete structure
Height	59.85m
Foundations, supporting stratum	Independent footing foundations, in-situ cast-in-place concrete pile with under-reamed pile GL-16m or deeper Tokyo sand and gravel strata
Framework	Column and beam moment resisting framework with buckling resistant vibration control braces (LY = 100N/mm ² class) and viscous vibration control walls
Facade	Glass curtain wall, PC panels

3. EARTHQUAKE OBSERVATION SYSTEM

The earthquake observation system consisted of accelerometers installed inside and outside the building (Fig. 5). Within the building, accelerometers were installed at a total of 11 locations: XYZ 3-component accelerometers were installed at five locations inside the services shaft from B1F to 14F, (Fig. 6). Outside the building, one accelerometer was installed near the ground surface (GL-1m) and one at the level of the tip of the piles (GL-16m) (engineering bedrock).

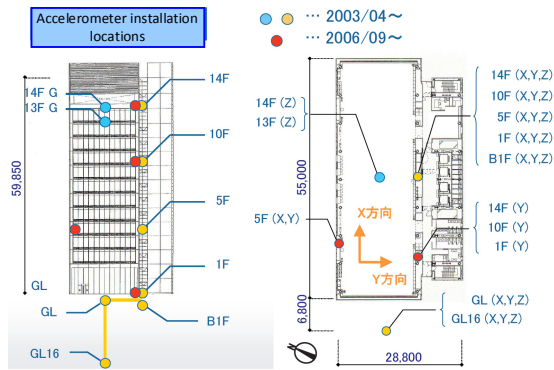


Figure 5. Earthquake observation system

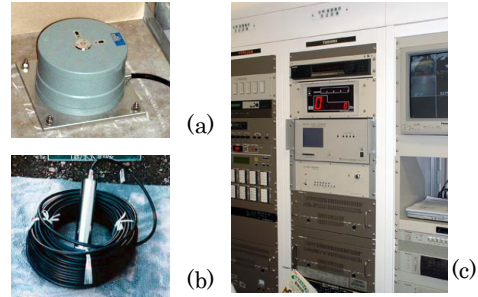


Figure 6. (a) Acceleration Sensor at EPS
(b) Acceleration Sensor at TOP of Pile
(c) Recording Apparatus

4. ANALYSIS OF THE EARTHQUAKE OBSERVATION RECORDS

4.1. The Main Shock at 2:47 p.m., March 11, 2011

- Measured earthquake intensity: Intensity V-upper (Chiyoda-ku, Tokyo)
- Recorded duration: 600 seconds
- Summary of damage: no damage to structure, finishing materials, or building equipment

4.2. Input Seismic Motions

Figure 7 shows the velocity response spectrum for the main shock at 2:47 p.m., March 11, 2011. The properties of a major earthquake having power in all period ranges can be seen, with seismic motions at periods of one second and longer virtually flat at around 30 cm/s. On the other hand, for periods shorter than one second, differences can be seen due to the differences in the position of installation of the accelerometers. The seismic motions increase in the order of pile tip (GL-16m), within the building (1F), and the ground surface (GL-1m). This is considered to be due to amplification of the soil strata near to surface in the case of the difference between pile tip and ground surface.

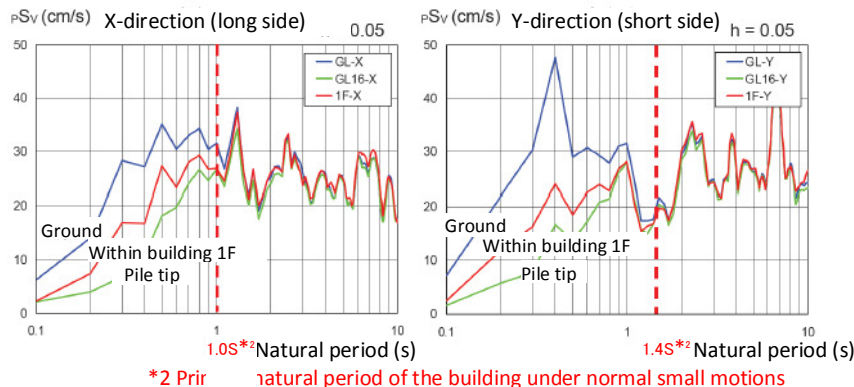


Figure 7. Velocity response spectra (2:47 p.m., March 11, 2011) (ground, pile tip, 1F)

4.3. Vibrations of the building (analysis according to maximum acceleration value)

Figure 8 shows the acceleration time wave form for the accelerometer installed within the core close to the position of the center of gravity of the building, and Fig. 9 shows the maximum values of acceleration in the height direction. In the distribution of acceleration in the height direction, the amount of amplification in the long side direction and the short side direction was different. This is considered to be due to the effect of the relationship between the seismic motions and the natural periods of the building. The vertical motions were about 0.4 to 0.53 times the horizontal motions. Also the vertical acceleration in the center of the large beam on 14F was 2.28 times the acceleration within the core, indicating that there was amplification.

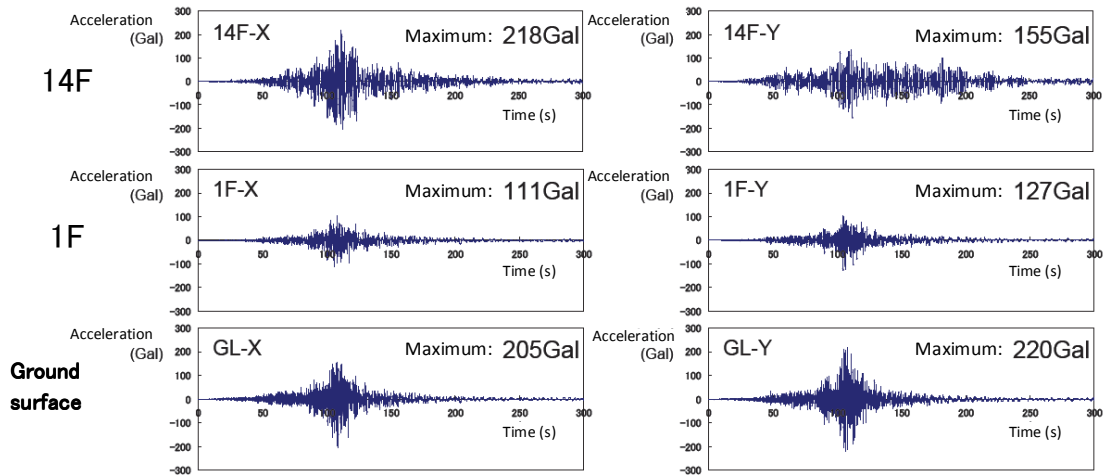


Figure 8. Acceleration waveforms for the core

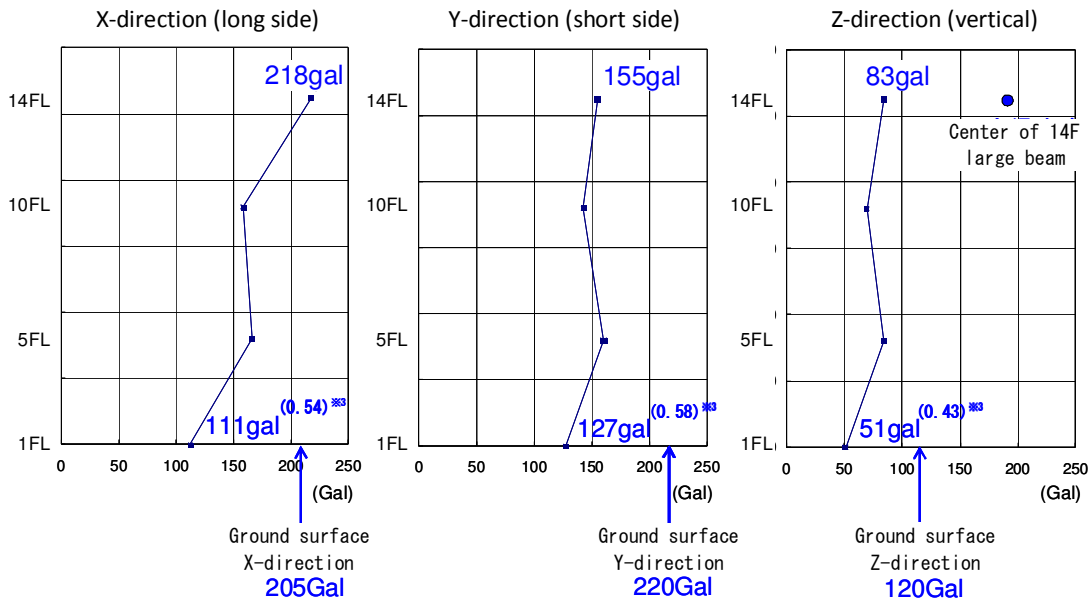


Figure 9. Maximum acceleration distribution (*3 indicates the ratio of 1F/ground)

4.4. Vibrations of the building (analysis according to maximum displacement)

The acceleration waveforms obtained were integrated to obtain deformations. The displacement time waveforms were calculated using third order spline interpolation between stories (Fig. 11). The overall displacements of the building were 76.1 mm, or 1/788 (long side, hereafter referred to as the X-direction), 69.8 mm (short side, hereafter referred to as the Y-direction) (Fig. 10), the maximum inter-story drift angle was 1/500 (X) (5F, inter-story displacement 8 mm), 1/667 (Y) (6F, inter-story displacement 6 mm), so estimating from the magnitude of the displacements no damage was expected, and a high level of seismic performance was confirmed (Fig. 11 and 12).

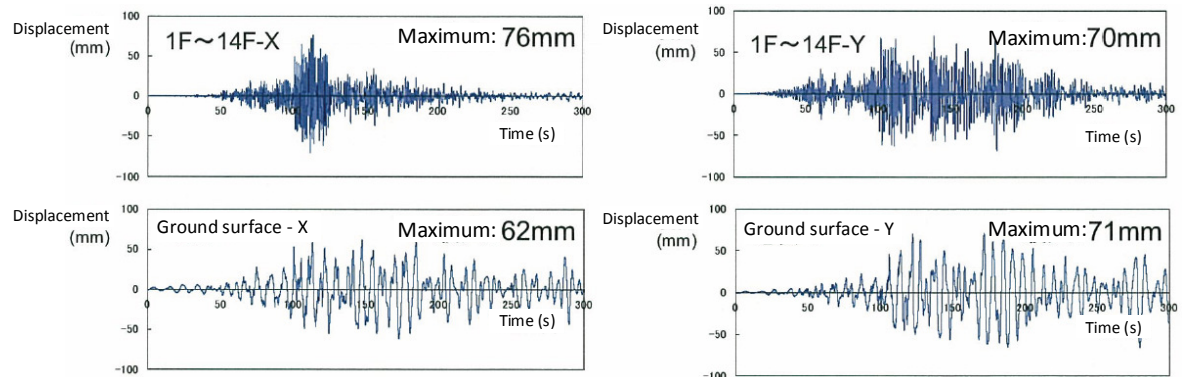


Figure 10. Displacement time wave form

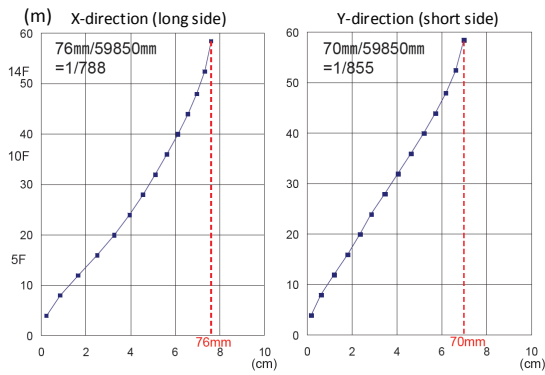


Figure 11. Maximum displacement (from 1F)

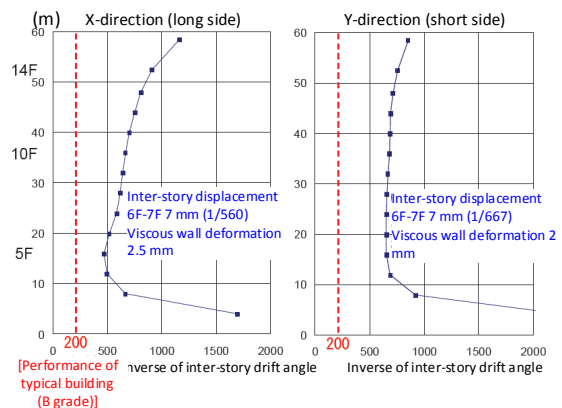


Figure 12. Maximum inter-story drift angle

4.5. Confirmation of performance as energy dissipation structure

In order to more accurately analyze the performance as a vibration control structure, the deformations of the energy dissipation members were directly measured (Fig. 13). The 6F vibration control members were measured at only four locations. Deformations of 2.52 mm (X) and 1.91 mm (Y) were measured on the viscous damping walls (Fig. 14). It is considered that the building as a whole absorbed seismic energy, and performed as an energy dissipation structure. Deformation of the structural steel energy dissipation braces was less than 1 mm (0.55 mm Y), so from this result it is considered that the performance was within the elastic range.

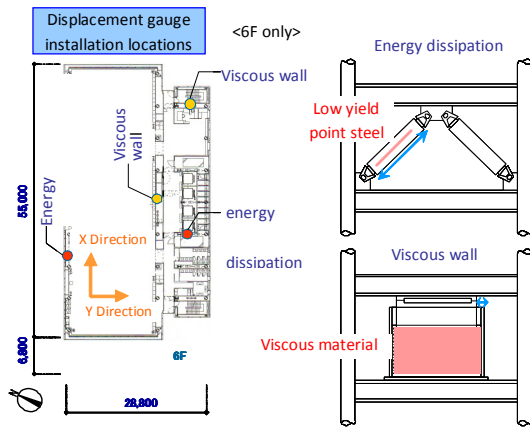


Figure 13. Displacement gauge installation locations

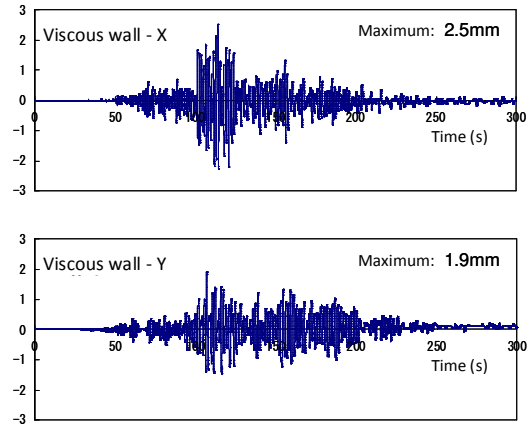


Figure 14. Viscous damping wall deformation

4.6. Changes in the natural period and damping factor

Figure 15 shows a comparison of the transfer function for the following three records: an earthquake that occurred in Sanriku-oki on March 9, 2011 (3/9 foreshock), the 3/11 main shock, and an aftershock that occurred two hours after the March 11 main shock. The transfer functions for the 14F with respect to the records for the 1F are shown for the X- and Y-directions. It can be seen that the two earthquakes apart from the main shock were small earthquakes from the fact that the values of the displacement at the top of the building were 5 mm and 10 mm. The natural period during the main shock on March 11 increased by 13 to 14% relative to the foreshock on March 9.

If the transfer ratio at the peak is considered to be proportional to the damping factor, then the natural frequency at the time of the March 11 main shock was reduced by 12 to 15% compared with prior to March 11, and the damping factor was increased by about a factor of two. Also, by comparing the March 9 foreshock and the March 11 aftershock it can be seen that there is a reduction in natural frequency. This is considered to be due to the internal and external finishing materials contributing to the stiffness of the building as a whole in addition to the structure. Also, the damping effect in the main shock was about double that in the two small earthquakes (4 to 6% damping factor), which confirms that the damping performance was exhibited.

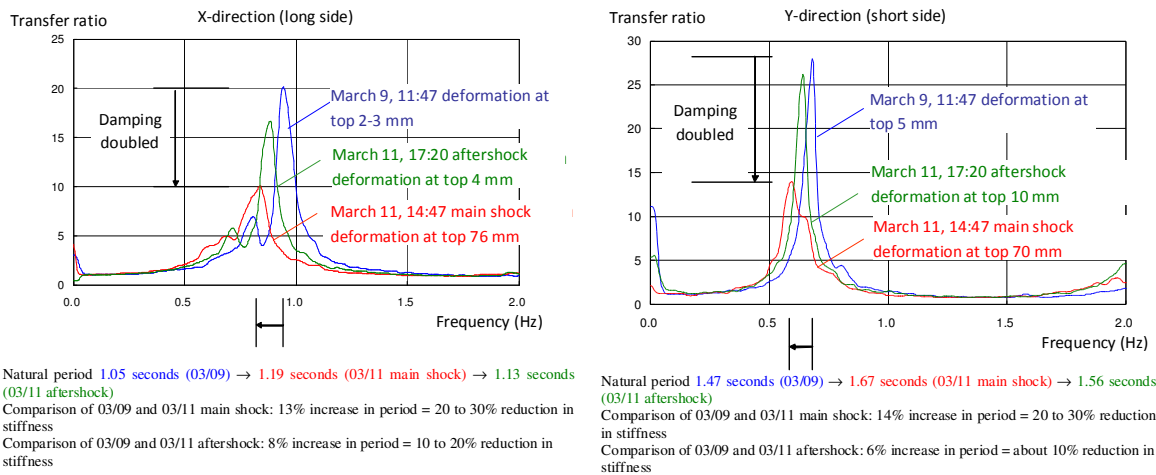


Figure 15. Change in the natural period and damping factor from the magnitude of the oscillations, and confirmation of vibration control structural performance

4.7. Dependence of damping factor and natural frequency on amplitude

Since starting measurement of earthquakes in April 2003, a total of 224 earthquakes has been recorded up to February 2012. The time recorded in the eight years from April 2003 until March 10, 2011 was 157 minutes. In contrast, the time recorded within one day from the main shock on 2:47 p.m., March 11, 2011 (hereafter abbreviated to 3/11 main shock) was 67 minutes, and within one month of the main shock was 105 minutes, and within one year of the main shock was 180 minutes. In other words, more records were obtained in 2011 than in the previous eight years.

Table 2. Number of earthquake records according to intensity for each year

	Intensity 1	Intensity 2	Intensity 3	Intensity 4	Intensity 5 weak	Intensity 5 strong	Total
2003 (from April)	3	7	5	0	0	0	15
2004	6	10	4	1	0	0	21
2005	16	9	6	1	0	0	32
2006	3	7	1	0	0	0	11
2007	2	3	1	0	0	0	6
2008	1	7	1	0	0	0	9
2009	1	1	2	0	0	0	4
2010	1	6	0	0	0	0	7
2011	22	68	16	1	0	1	108
2012 (to February)	5	4	2	0	0	0	11

All the records obtained since the start of measurement were divided into before and after the 3/11 main shock, and the damping factor was estimated using the half power method. Figures 16 and 17 plot the damping factor against displacement of the top of the building in the X- and Y-directions. Although the values themselves were evaluated slightly higher, a trend indicating a larger damping factor the larger the response amplitude was confirmed.

On the other hand, Figs. 18 and 19 plot the results with the frequency at the point of the peak in the transfer function taken to be the natural frequency. From these figures a clear difference between before and after 3/11 can be seen. The natural frequencies in both the X- and Y-directions after 3/11 are considered to be reduced by about 10%. It is considered that this was caused by the stiffness reduction of the filling materials and sealing materials between finishing materials or between finishing materials and the structure.

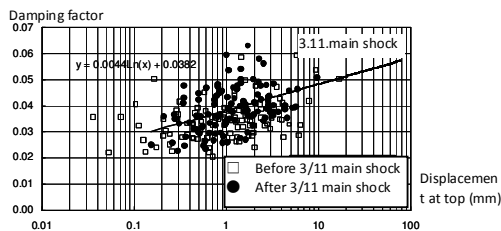


Figure 16. Dependence of X-direction primary damping factor on amplitude

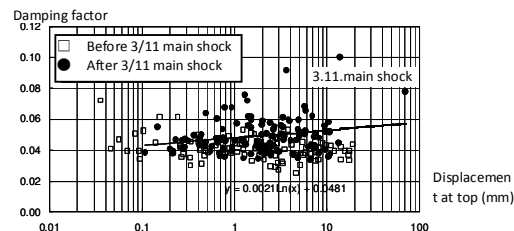


Figure 17. Dependence of Y-direction primary damping factor on amplitude

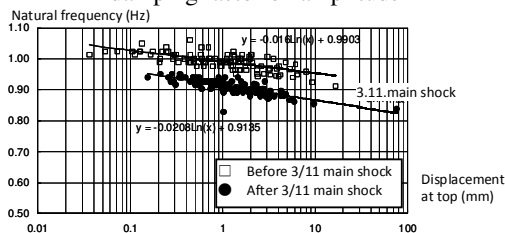


Figure 18. Dependence of X-direction primary natural frequency on amplitude

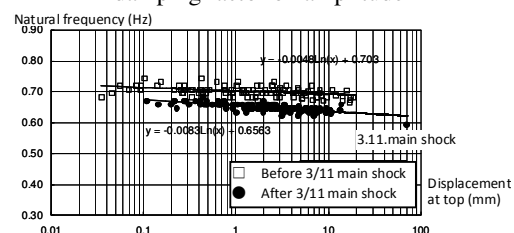


Figure 19. Dependence of Y-direction primary natural frequency on amplitude

5. ANALYSIS USING VIBRATION ANALYSIS MODEL

5.1. Design model

The design model is a three-dimensional vibration analysis model that evaluates all the members, B1F and 1F are fixed in the horizontal directions (X and Y), and vertical springs are provided at the pile caps to take in consideration loads in the vertical direction (Fig. 21). It was assumed that there is a stiff floor on each story, and that the vibrational degrees of freedom having mass and rotational inertia are concentrated into 3 degrees of freedom (X, Y, and θ_z) at the center of gravity of each story.

$$F_w = C_w \cdot V_e^K + K_w \delta_e \quad (1)$$

The internal viscous damping was set to be proportional to the initial stiffness, and the damping factor was taken to be 2% of the primary natural period.

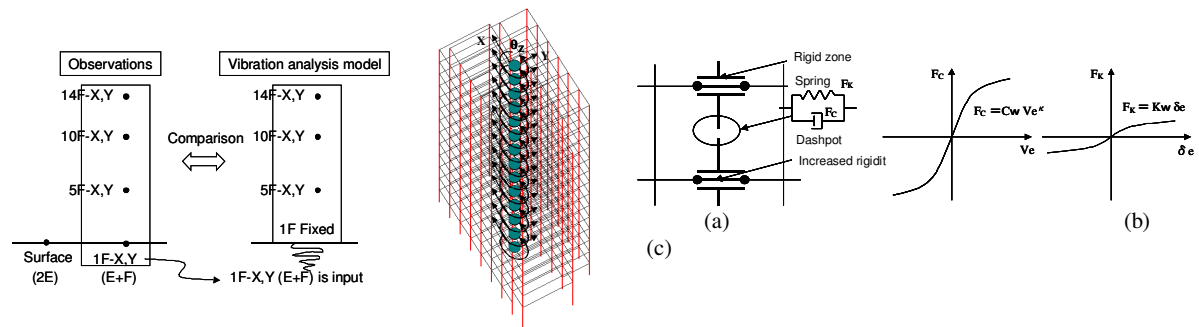


Figure 20. Relationship of Observed and Analytical Vibrations **Figure 21.** Vibrational Analysis Model **Figure 22.** Modeling of Viscous Damping Walls

5.2. Comparison of measurement results and analysis results of the design model

Vibration analysis was carried out on the three-dimensional vibration analysis model (design model) inputting the XY-direction components (X, Y) of the 3/11 main shock and the 3/11 aftershock acceleration records. The accuracy of the design model was verified by comparing the transfer function obtained from the 14F analysis results with respect to 1F with that of the earthquake records.

5.2.1. Comparison of transfer functions (14F/1F input acceleration)

Figures 23 to 26 show the transfer functions in the X- and Y-directions for 14F response accelerations with respect to 1F accelerations; Fig. 23 is for the 3/11 main shock input to the design model, Fig. 24 is for the 3/11 main shock, Fig. 25 is for the 3/11 aftershock input to the design model, and Fig. 26 is for the 3/11 aftershock. The predominant frequencies of design model and the 3/11 main shock are virtually the same, indicating that evaluation of the stiffness of the design model was highly accurate. On the other hand, the value of the predominant frequency of the 3/11 aftershock was slightly on the high-frequency side compared with the design model. The deformation of the top of the building in the 3/11 aftershock was small at 2.7 mm (X) and 7.0 mm (Y), so there was no reduction in stiffness of the internal and external finishes, so it is considered that the frequency was high compared with the 3/11 main shock. From the above it was confirmed that the design model is capable of appropriately evaluating the stiffness in earthquakes with amplitude levels similar to those of the 3/11 main shock. The value of the amplification ratio from the design model was generally greater than the measured records. It is considered that if the actual behaviour is estimated based on the design model, there is an overall tendency to under-evaluate the damping, so the evaluation of the design model is on the safe side.

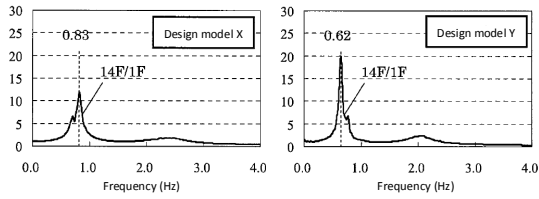


Figure 23. Design model transfer functions (3/11 main shock input)

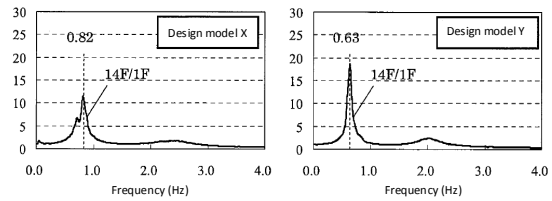


Figure 25. Design model transfer functions (3/11 aftershock input)

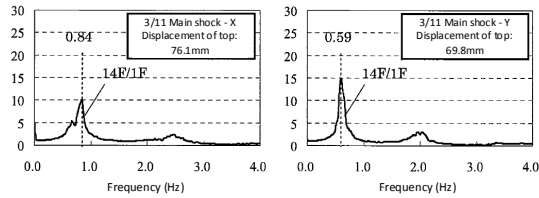


Figure 24. Transfer functions for 3/11 main shock (2:47 p.m. 2011/3/11)

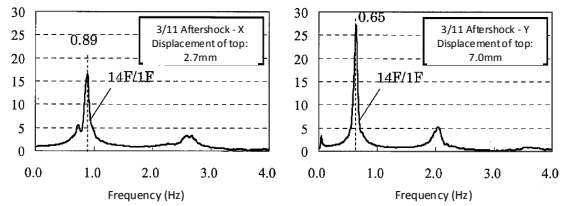


Figure 26. Transfer functions for 3/11 aftershock (4:29 pm, March 11, 2011)

5.2.2. Comparison of response results

(maximum displacement, inter-story drift angle, maximum acceleration)

Figures 27 to 30 show a comparison of the measured earthquake records and the design model response analysis results for the 3/11 main shock. It can be seen that the vibration analysis using the design model can generally reproduce the measured results.

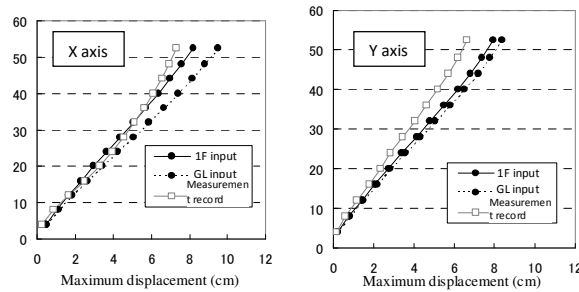


Figure 27. Maximum displacement

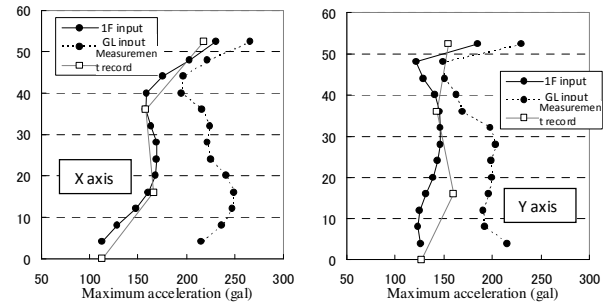


Figure 29. Maximum floor response acceleration

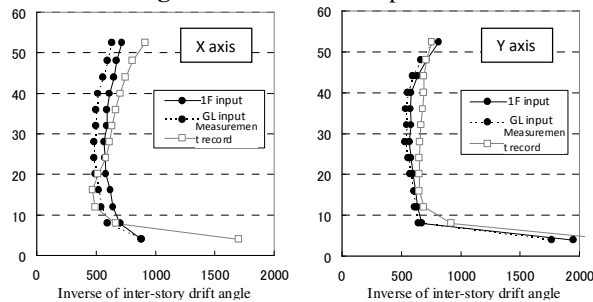


Figure 28. Maximum inter-story drift angle

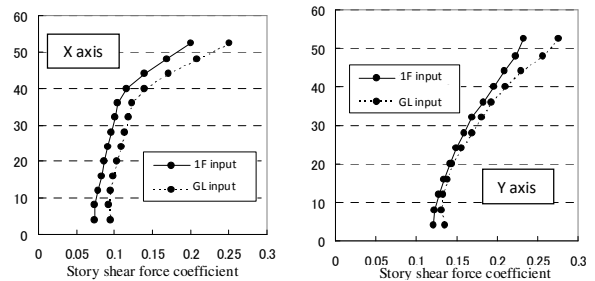


Figure 30. Story shear force coefficient

5.2.3. Comparison of the differences due to input

Figures 25 to 29 also show the results when the ground surface (GL) seismic record for the 3/11 main shock was input to the design model. As shown in Table 1, when a comparison of the input earthquake measurement points 1F and GL for 1F story shear force coefficient is carried out, differences in input acceleration of 0.54 (X), and 0.58 (Y) were obtained. In contrast for the story shear force coefficient, differences of 0.81 (X) and 0.88 (Y) were obtained. From this it can be seen that the effect on the story shear force was smaller compared with the reduction in input acceleration.

Table 3 comparison of input acceleration and stories shear force coefficient

	X-direction		Y-direction	
	Input acceleration (gal)	Story shear force coefficient	Input acceleration (gal)	Story shear force coefficient
1F input	111	0.07	127	0.12
GL input	205	0.09	220	0.135
1F/GL	0.54	0.81	0.58	0.89

6. CONCLUSION

The following is a summary of the results of the investigation using the measured seismic records from The Great East Japan Earthquake of March 11, 2011 and a subsequent aftershock.

- The high seismic performance envisaged during the design was confirmed from the measurement results for the main earthquake which was intensity V-upper.
- For these seismic motions the viscous damping walls absorbed the seismic energy of the building so that the effect as a energy dissipation structure was exhibited. The structural steel braces were within the elastic range.
- It was found that the natural frequency depends on the amplitude. The frequency in the main shock was reduced by about 10% compared with small earthquakes. This is considered to be due to the effect of reduction in stiffness of the nonstructural internal and external finishing members.
- It was confirmed that the analysis model used during the design agreed with the measurement results in the main shock.

REFERENCES

Hiroaki Harada, Masato Ishii; A Study on dynamic behaviour of passive energy dissipation systems based on seismic observation records: Part 1, Part 2 - 9th World Seminar Isolation, Energy Dissipation and Active Vibration Control of Structures, Japan, June 13-16, 2005.